Cancer Immunology, Immunotherapy (2025) 74:200
https://doi.org/10.1007/s00262-025-04065-5

RESEARCH

# Characterization of the aryl hydrocarbon receptor as a potential candidate to improve cancer T cell therapies

**Valentine De Castro[1] · Oumaïma Abdellaoui[1] · Barbara Dehecq[1] · Babacar Ndao[1] · Patricia Mercier-Letondal[1] · Alexandra Dauvé[2] · Francine Garnache-Ottou[1,3] · Olivier Adotévi[1,4] · Romain Loyon[1] · Yann Godet[1]**

Received: 30 September 2024 / Accepted: 15 April 2025


**Abstract**
The efficacy of T-cell-based cancer therapies can be limited by the tumor microenvironment which can lead to T cell dysfunction. Multiple studies, particularly in murine models, have demonstrated the capacity of the aryl hydrocarbon receptor (AHR) to negatively regulate antitumor T cell functions. AHR is a cytoplasmic receptor and transcription factor that was originally identified as a xenobiotic sensor, but has since been shown to play a significant role in the gene regulation of various immune cells, including T cells. Given the insights from murine studies, AHR emerges as a promising candidate to invalidate for optimizing T cell-based cancer therapies. However, the controversial role of AHR in human T cells underscores the need for a more comprehensive characterization of AHR expressing T cells. This study aims to investigate the regulatory mechanisms of AHR in human T cell biology to better understand its impact on reducing antitumor immune responses. Here, we knocked-out AHR in human T cells using CRISPR-Cas9 technology to characterize AHR's function in an in vitro chronic stimulation model. Engineered T cells exhibited enhanced effector- and memory-like profiles and expressed reduced amount of CD39 and TIGIT. *AHR* knockout enhanced human CAR-T cells' functionality and persistence upon tumor chronic stimulation. Collectively, these results highlight the role of AHR in human CAR-T cells efficiency.

**Keywords** AHR · T cell dysfunction · CRISPR-Cas9 · CAR-T cell therapy

## Introduction

CAR-T therapy is a therapeutic strategy that has demonstrated encouraging clinical responses, notably in the targeting of refractory and relapsed hematological malignancies. Currently, six medications have been approved by public health authorities for the treatment of B cell acute lymphoblastic leukemia, lymphomas, and multiple myeloma. These medications established CAR-T therapy as one of the most promising approaches to treat cancer so far [1]. However, despite the remarkable responses observed, a substantial number of patients either do not respond, or relapse, and the targeting of solid tumors remains challenging. These challenges can be attributed to the several inherent limitations of CAR-T therapy, such as the immunosuppressive tumor microenvironment and chronic antigen exposure, which can lead to T cell dysfunction [2].

To overcome these obstacles, different groups have focused on the CRISPR-Cas approach with the idea of invalidating factors that may be involved in the establishment or maintenance of the dysfunctional T cell state. This state is characterized by impaired proliferation and effector capacities, heightened expression of inhibitory receptors, as well as distinct transcriptomic, epigenetic, and metabolic profiles [3]. Here, we focused on the aryl hydrocarbon receptor (AHR), a cytoplasmic receptor and transcription factor activated by a plethora of ligands found within tumors. This receptor is therefore crucial for various biological processes, including responses to xenobiotics, drug metabolism, and immune responses [4]. In the context of antitumor immunity, AHR has been shown to influence

✉ Yann Godet
yann.godet@univ-fcomte.fr

1 Université Marie et Louis Pasteur, EFS, INSERM UMR1098 RIGHT, 25000 Besançon, France

2 MGX-Montpellier GenomiX, Université de Montpellier, CNRS, INSERM, Montpellier, France

3 Service d'hématologie et d'immunologie cellulaire, Centre Hospitalier Universitaire de Besançon, Besançon, France

4 Service d'oncologie médicale, Centre Hospitalier Universitaire de Besançon, Besançon, France

Published online: 13 May 2025

the polarization of immunosuppressive regulatory T cells ($T_{reg}$) and type 1 regulatory T cells ($T_{r1}$) [5, 6] leading to immunosuppressive microenvironment within tumors. Moreover, AHR has been described as being involved in the inhibition of antitumor T cells functions [7, 8]. AHR is also pivotal in various immunosuppressive pathways, including the IDO/kynurenine axis. Indeed, AHR acts as the principal receptor of kynurenine [6], a tryptophan-derived immunosuppressive molecule metabolized by IDO1/2 and TDO2 enzymes, known to be overexpressed in cancers associated with poor prognoses [9]. Upon activation by kynurenine, AHR has also been shown to be implicated in the CD39/CD73/adenosine/A2AR axis by regulating the expression of CD39 [10]. These insights underscore the multiplicity of the role of AhR in T cell regulation and highlight its potential as a target for enhancing antitumor immunity. To determine whether targeting AHR could be an interesting strategy to enhance adoptive T cell therapy, *AHR* knocked-out T cells were characterized for some of the previously described dysfunctional features.

## Methods

### Cell line

The human blastic plasmacytoid dendritic cell neoplasm cell line CAL-1, naturally expressing the CD123 antigen, was obtained from Dr Maeda (University of Nagasaki, Japan; RRID: CVCL_5G46) and maintained in culture in RPMI-1640 medium (Gibco, 14,540,122) supplemented with 10% FBS (Gibco, 10,270,106) and 1% penicillin–streptomycin (Gibco, 15,140,122). The cell line was cultured in a 37 °C incubator saturated with water vapor containing 5% $CO_2$. The cell line was checked for the absence of mycoplasma and for its identity before being achieved in a master cell bank.

### T cell collection, activation, and expansion

Peripheral blood was collected from healthy donors of different ages and genders without any distinction at the Etablissement Français du Sang (EFS) as apheresis kit-preparations after obtaining informed consent and following internal guidelines. Mononuclear cells were isolated by centrifugation on a Ficoll gradient (Eurobio, CMSMSL01-01), and activated using anti-CD3/CD28 microbeads (Thermofisher, 111.31D) according to the manufacturer's instructions. Beads-attached T cells were magnetically isolated and cultured in RPMI-1640 medium supplemented with 10% human serum (locally produced by EFS) and 1% penicillin–streptomycin, in the presence of IL-2 500 IU/mL (Novartis, Proleukin®).

### Lentivirus production and transduction

Third-generation CD123 CAR has been described in previous studies [11]. Lentivirus encoding the CAR was obtained from the supernatant derived from HEK-293T packaging cell line. Briefly, cells were plated one day before co-transfection using the necessary CAR vector, psPAX (RD-Biotech, lot no. 230420LNe_psPAX2) and pMD2G (RD-Biotech, lot no. 230420LNe_pMD2G) plasmids in a medium enriched with calcium phosphate (Thermofisher, J63122.AD). Medium was replaced with fresh OPTI-MEM® (Gibco, 31,985,070) 24 h after. Supernatant was harvested 48 h later using a centrifugal filter (Sigma Aldrich, UFC910024) for concentration and purification according to the manufacturer's instructions. Supernatant titration was performed to adjust the multiplicity of infection (MOI) using HEK-293T cells, which were put in culture with different dilutions of the lentiviral vector ranging from 1:10 to 1:1 000. Percentage of HEK-293T cells expressing the CD19 selection marker was then assessed by flow cytometry. T cells were transduced two days post-activation at a MOI of 3, and transduction efficiency was determined based on CD19 expression.

### CRISPR-Cas9-mediated gene editing

CRISPR-Cas9 gene editing was performed by electroporating sgRNA/Cas9 ribonucleoprotein (RNP) complex using the 4D-Nucleofector System N (Lonza) and the Primary cell 4D-nucleofector kit (V4XP-3032, Lonza). RNP containing 40 µM Cas9 protein (Integrated DNA Technologies, Alt-R S.p. HiFi Cas9 Nuclease V3, 1,081,060) and 80 µM sgRNA targeting *AHR* (Integrated DNA Technologies, Custom Alt-R CRISPR-Cas9 sgRNA, 5′-GGCCTCCGTTTCTTTCAGTA-3′) or a scramble sgRNA, were complexed for 30 min at room temperature. Three days post-activation, $1 \times 10^6$ T cells or $2 \times 10^5$ CAR-T cells after 24 h of lentiviral transduction were centrifuged at 200 g for 10 min and re-suspended in 20 µL of transfection buffer and RNP. The mixture was transferred into the electroporation cuvette using the EO-115 program in 16-well cuvette strips. The cells were then recovered in preheated T cell medium and expanded as described above.

### Flow cytometry analysis

Flow cytometry was performed using the LSR Fortessa (BD Biosciences) and CytoFLEX (Beckman) cytometers

**Table 1** Antibodies resources

| Antibodies | Source | Identifier Cat# |
|---|---|---|
| CD3 BV421 | BD Biosciences | 562426 |
| CD3 FITC | BD Biosciences | 555332 |
| CD8 BV510 | BD Biosciences | 563919 |
| CD8 PE-Cy7 | BD Biosciences | 557746 |
| IFN-γ BV421 | BD Biosciences | 562988 |
| Isotype mouse IgG1κ BV421 | BD Biosciences | 562438 |
| IL-2 PE | BD Biosciences | 560709 |
| Isotype rat IgG2aκ PE | BD Biosciences | 555844 |
| CD107a PE | BD Biosciences | 555801 |
| Isotype mouse IgG1κ PE | BD Biosciences | 555749 |
| TIGIT BV421 | BD Biosciences | 747844 |
| Isotype mouse IgG2κ BV421 | BD Biosciences | 562748 |
| CD39 PerCp-Cy5.5 | BD Biosciences | 564899 |
| Isotype mouse IgG2b PerCp-Cy5.5 | BD Biosciences | 558304 |
| 7-AAD | BD Biosciences | 559925 |
| CD19 APC | Sony Biotechnology | 2111060 |
| CD123 PE-Cy7 | Sony Biotechnology | 2130050 |
| TNF-α BV510 | Sony Biotechnology | 3114750 |
| Isotype mouse IgG1κ BV510 | Sony Biotechnology | 2600860 |
| Fixable viability dye eFluor 780 | eBioscience | 65-0865-14 |

with the antibodies listed in Table 1. Data were analyzed using FlowJo™ v10.8 Software (BD Life Sciences).

For cytokine production analysis, T cells were stimulated with 25 ng/mL phorbol 12-myristate 13-acetate (Sigma Aldrich, P8139) and 1 µg/mL ionomycine (Sigma Aldrich, 10,634), while CAR-T cells were put in co-culture with their tumor target. Both were stimulated for 5 h in the presence of GolgiPlug® (BD Biosciences, 555,020). Cytokine detection was performed after fixing and permeabilizing cell membrane using the BD Cytofix/Cytoperm™ kit (BD Biosciences, 555,028), following the manufacturer's instructions.

For the CD107a degranulation assay, CAR-T cells were put in co-culture with their tumor target for 5 h, in the presence of GolgiStop® (BD Biosciences, 554,724) and anti-CD107a antibody.

## Western blot analysis

Cell lysates were obtained using RIPA lysis buffer (Sigma Aldrich, R0278). After diluting the protein fractions in 2X Laemmli buffer, the lysates were separated by SDS-PAGE (7.5% Acrylamide, 100–150 V). The proteins in the gel were then transferred to previously activated PVDF membranes using 1X transfer buffer (2.5 mM Tris, 19.2 mM Glycine, H2O qs 1 L, 100 V). After saturation with a solution of 5% skimmed milk (w/v)-Tween20 0.1%-TBS 1X, the membranes were incubated for 1 h at 4 °C. The membranes were then washed and brought into contact with primary antibodies anti- AHR (Cell Signaling, 83200S) or anti-β-actin (Sigma Aldrich, A5441, RRID:AB_476744) diluted 1:40,000. After washing the membranes, they were incubated in the presence of anti-rabbit (BD Biosciences, 554,021, RRID:AB_395213) and anti-mouse (BD Biosciences, 554,002, RRID:AB_395198) secondary antibodies diluted 1:1,000. The fixation of the secondary antibodies was detected using the ECL Bio-Rad mixture (Peroxide reagent and Lumminol, v/v) and signals were measured using the Chemidoc XRS device.

Subcellular localization was performed after 24 h of stimulation, followed by treatment with 50 µM kynurenine for 30 min. Subcellular fractionation was conducted using the NE-PER™ Cytoplasmic and Nuclear Extraction Reagent Kit (Thermofisher, 78,833) according to the manufacturer's recommendations. Subcellular localization was then analyzed by Western Blotting. The purity of each fraction was assessed using anti-β-tubulin (Cell Signaling Technology, 2128) and anti-H3 histone (Cell Signaling Technology, 4499) antibodies.

## Cytotoxicity assays

The cytotoxicity was assessed after staining effector cells with a cell proliferation dye eFluor 450 solution (Invitrogen, 65-0842-85) in accordance with the manufacturer's instructions. The cells were put in co-culture with their tumor target at the indicated effector:target ratio of 1:1 or 1:10 for 24 h. The percentage of cytotoxicity was evaluated using TruCount™ tubes (BD Biosciences, 663,028).

### T cell and CAR-T cell stimulation assays

T cells were stimulated once or four times every 2–3 days with anti-CD3/CD28 microbeads, with or without 50 µM kynurenine (Invivogen, tlr-kyn). Before each stimulation, beads were removed and replaced with a new batch. CAR-T cells were put in co-culture with a tumor cell line at an effector:target ratio of 1:15 for 7 days in a volume of 1,5 mL. Every 3–4 days, 500 µL of RPMI-1640 medium was replaced with fresh medium.

### Quantitative real-time PCR

Gene expression was assessed 48 h after the first and fourth stimulations. Cells were lysed and RNA was extracted using an extraction kit (Macherey Nagel, 740,955-250) according to the manufacturer's instructions, before being quantified using the Nanodrop 2000 Spectrophotometer (Thermofisher). Then, cDNA was synthesized using the PrimeScript™ RT Master Mix RT-PCR kit (Takara, RR036A) following the manufacturer's recommendations. Quantitative PCR was carried out using primers targeting the genes *AHR* (Thermofisher, Hs00169233_m1), *CYP1A1* (Thermofisher, Hs01054797_g1), *TBX21* (Thermofisher, Hs00203436_m1), *TCF7* (Thermofisher, Hs01556515_m1), *EOMES* (Thermofisher, Hs00172872_m1), *SELL* (Thermofisher, Hs01547250_m1), *TGFB1* (Thermofisher, Hs009981338_m1), *IL10* (Thermofisher, Hs00961622_m1) and *18S* (Thermofisher, Hs03003631_g1). qPCR was carried out using Taqman™ Universal Master Mix II (Thermofisher, 4,440,038). The acquisition was carried out within the Biorad qPCR thermal cycler. Transcript levels were normalized to 18S RNA using the $2^{-\Delta\Delta Ct}$ method.

### RNA-sequencing

In order to analyze different gene expressions, total RNA was extracted using the Machery Nagel extraction kit according to the manufacturer's recommendations. The quantity of extracted RNA was evaluated using the Nanodrop 2000 Spectrophotometer, and sample purity was evaluated using the 2100 Bioanalyzer (Agilent) with the RNA 6000 Pico Kit for 2100 Bioanalyzer Systems. cDNA libraries were constructed using the Stranded mRNA Prep Ligation kit (Illumina) and sequenced from both ends with each read being 50 nucleotides in length. Sequencing was performed on an SR100/PE501 lane using the NovaseqSP1 system (Illumina). Sequences were quality checked using FASTQC (v0.11.9). Low quality bases (Phred quality score less than 30) were filtered out and adapters were trimmed using trimmomatic (v0.39). Reads were mapped to GRCh38 using STAR (v2.7.8a) with count reads per gene. The aligned reads were summarized at the gene-level using the function featureCounts of Subread (v2.0.1). Counts were normalized by the size of corresponding library (DESeq2, estimateSizeFactors function). Differentially expressed genes (DEG) analysis was performed using DESeq2 package with default parameters. Genes were considered as DEG if they achieved a false discovery rate of 5% or less and a fold change of 2 ($-1 < \log2Foldchange > 1$). Gene annotation was carried out using Homo sapiens (org.Hs.eg.db) AnnotationDbi from R/Bioconductor. Gene Set Enrichment Analysis was performed using clusterProfiler (v4.0). Briefly, all statistically enriched terms were identified (GO/KEGG terms, canonical pathways), then accumulative hypergeometric *p*-values and *q*-values are calculated using the Benjamini–Hochberg procedure to account for multiple testings and enrichment factors were calculated and used for filtering. Computations have been performed on the supercomputer facilities of the Mésocentre de calcul of Franche-Comté.

The RNA-seq dataset is deposited in the NCBI Gene Expression Omnibus under accession code GSE279526.

### Statistical analysis

Student *t* tests (with Welch's correction when unequal variances) or Wilcoxon tests were performed using the GraphPad Prism 10.1.1 software (GraphPad Software), depending on the data distribution (i.e. normal or non-normal distribution). Samples were considered as paired and two-tailed tests were performed. *P* values $< 0.05$ were considered to be statistically significant ($*p < 0.05$, $**p < 0.01$, $***p < 0.001$, $****p < 0.0001$).

## Results

### AHR is induced upon T cell activation and is maintained over time upon chronic stimulation

First, an evaluation of the AHR expression within activated T cells was done by Western Blotting, revealing an induction of AHR expression upon T cell activation Indeed, *AHR* expression reached a maximum 3 days after T cells activation, which was followed by a decrease reaching a minimum 6 days after T cells activation. (Fig. 1a). Subsequent subcellular localization confirmed AHR activation by the kynurenine agonist, as demonstrated by AHR translocation from the cytosol to the nucleus (Fig. 1b). Next, to mimic chronic antigenic stimulation that occurs in the tumor microenvironment, T cells were stimulated chronically in vitro through TCR activation (Fig. 1c). The application of this protocol revealed that AHR expression was sustained throughout chronic stimulations, with no

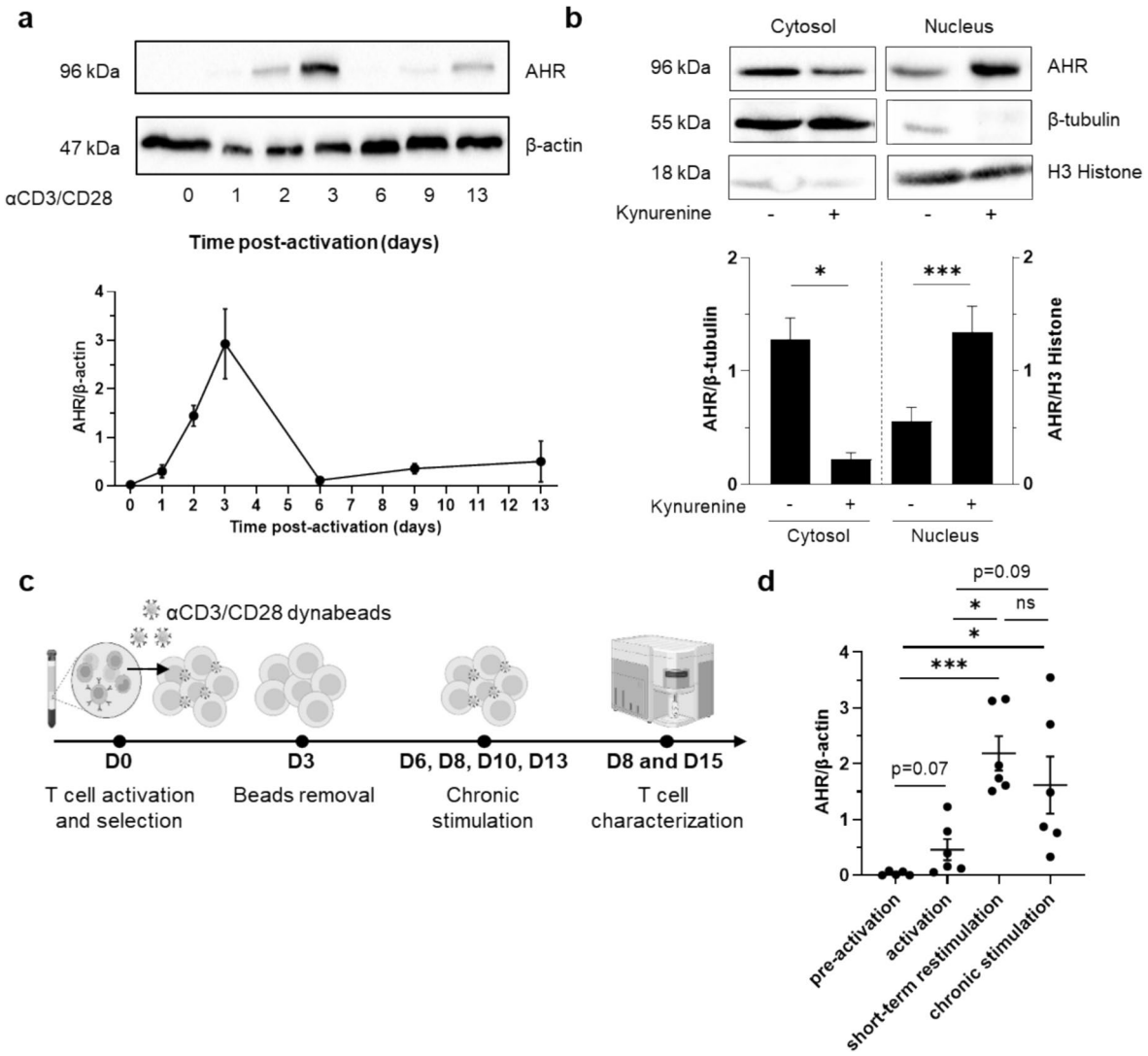


**Fig. 1** AHR is induced upon T cell activation and is maintained over time upon chronic stimulation. **a** Follow-up of AHR protein expression over time in activated T cells. (n = 2 to 7 according to timepoints) **b** Subcellular localization of AHR after treatment with 50 µM of kynurenine. (n = 8) **c** Methodology of in vitro chronic stimulation assay consisting of a chronic stimulation with αCD3/CD28 dynabeads. **d** Follow-up of protein AHR expression prior to T cell activation and after short-term restimulation (T cells restimulated once) or chronic stimulation (T cells restimulated four times). (n = 4 (non-restimulated), n = 28 (short-term restimulation), n = 5 (chronic stimulation))

significant difference being observed when comparing T cells subjected to short-term restimulation and T cells subjected to chronic stimulation. These findings suggest that AHR is highly expressed upon T cell restimulation (Fig. 1d).

## In vitro chronic stimulation induces a T cell dysfunctional state

The effects of chronic stimulation were initially evaluated in terms of T cell proliferation capacity as well as their viability. Based on this, a significant delay in proliferation and a reduction in viability were observed upon stimulation (Fig. 2a, b). To further characterize these observations, RNA sequencing analysis was performed after short-term restimulation or chronic stimulation. Principal component analysis revealed two distinct clusters following short-term restimulation or chronic stimulation (Fig. 2c). As expected, differential gene expression analysis reported a heightened expression of exhausted-like markers in chronically stimulated T cells (Fig. 2d). Additionally, the effect of chronic stimulation was also studied by measuring the inhibitory receptors' protein expression. The percentage of CD39 and the co-expression of PD-1/TIM-3 as well as PD-1/TIGIT did not increase in unstimulated T cells over time. In contrast, chronically stimulated T cells showed a progressive increase of these markers (Fig. 2e–g). Altogether, chronic in vitro stimulation of

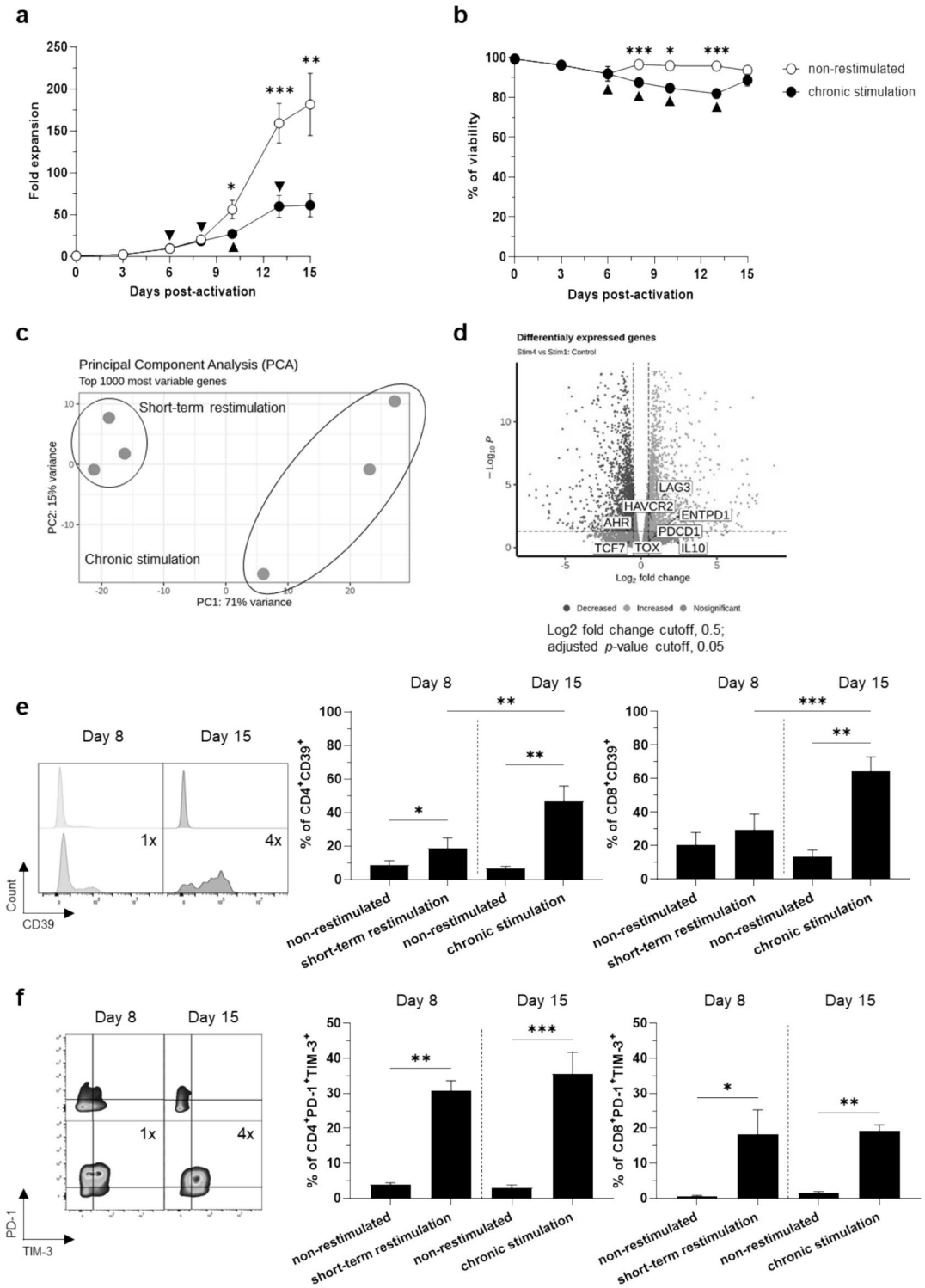


**Fig. 2** In vitro chronic stimulation induces a T cell dysfunctional state. **a**, **b** Follow-up of the proliferation (**a**) and viability (**b**) of T cells chronically stimulated and treated with 50 µM of kynurenine. (n = 9) **c** Principal Component Analysis (PCA) plot illustrating the distribution of T cells stimulated once or four times in the first two principal components (PC1 and PC2). (n = 3) **d** Volcano plot displaying the differential expression of genes between T cells stimulated once or four times. (n = 3) **e**–**g** CD39, PD-1, TIM-3 and TIGIT expression after short-term restimulation (T cells restimulated once) or chronic stimulation (T cells stimulated four times). (n = 9 (**e**), n = 12 (**f, g**)) **h** Knockout validation of *AHR* in activated T cells. (n = 10 (non-stimulated), n = 28 (short-term restimulation), n = 5 (chronic stimulation)) **i**, **j** Follow up of the proliferation (**i**) and viability (**j**) of *AHR* knocked-out T cells treated with 50 µM of kynurenine. (n = 6)

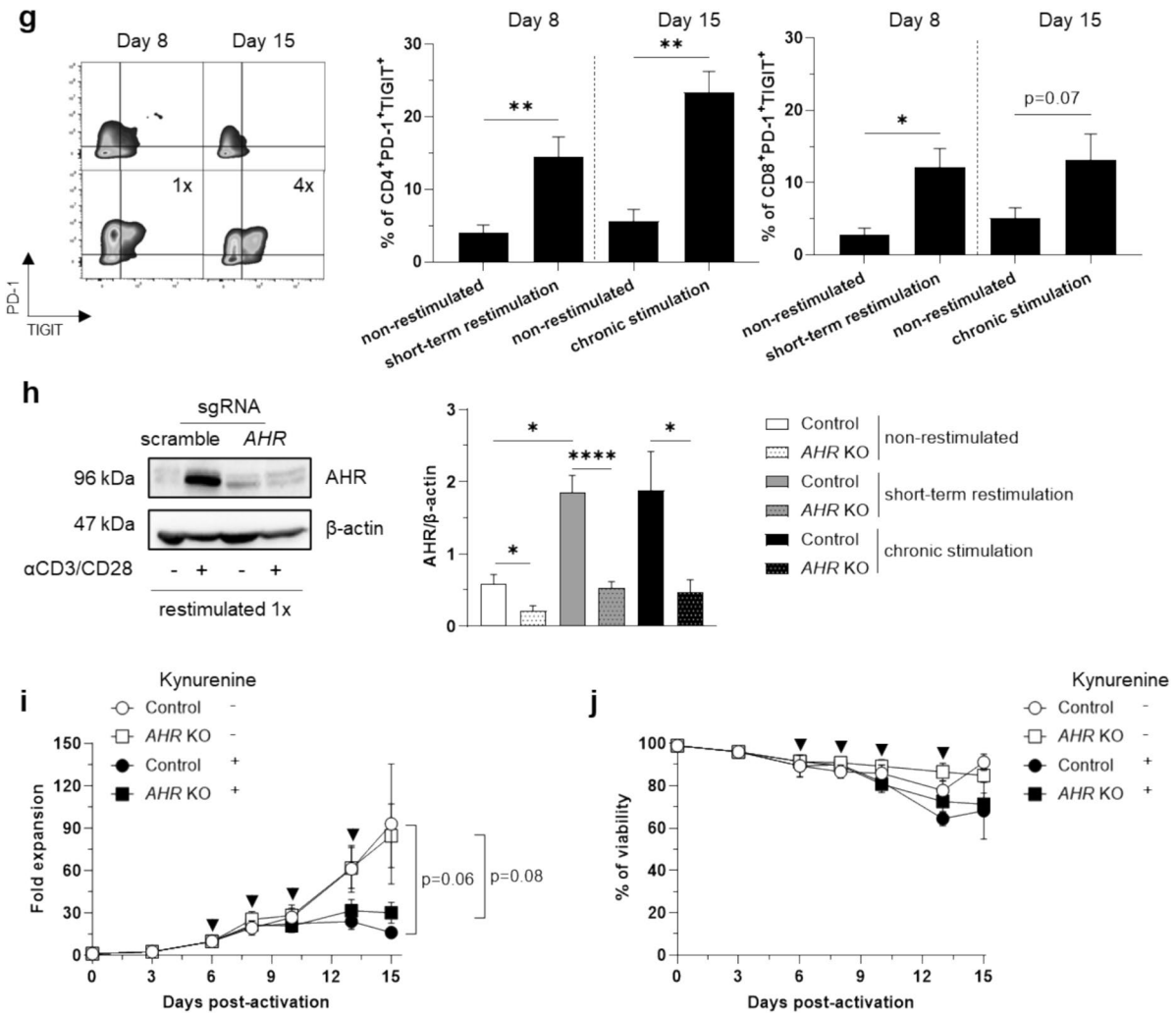


**Fig. 2** (continued)

T cells gradually diminished their proliferative capacities and viability, while also leading to an increase in cells expressing inhibitory receptors, which is characteristic of an exhausted-like phenotype (Fig. 2a–g). Thereafter, *AHR* knocked-out T cells were engineered using CRISPR-Cas9 technology. The sgRNA was designed using the CRISPOR.org web tool and achieved an editing efficiency of approximately 80% three days after the knock-out (Fig. 2h). Chronic stimulation and kynurenine treatment of these engineered T cells induced a decrease in proliferation capacity and viability, indicating a deleterious effect of kynurenine, even when *AHR* is knocked-out (Fig. 2i, j).

## *AHR* knockout promotes effector- and memory-like profiles upon T cell stimulation

To further investigate the impact of *AHR* knockout on T cells differentiation, RNA-sequencing was performed in the presence of kynurenine after short-term restimulation (Fig. 3a). The downregulation of *CYP1A1*, *CYP1B1* and *AHRR*, known to be regulated by AHR, confirmed the robustness of the RNA-sequencing data (Fig. 3b). Pathway analysis revealed that immune effector processes and T cell activation pathways were enriched in *AHR* knocked-out T cells (Fig. 3c). Indeed, effector-associated genes were up-regulated in the knockout condition and there was a higher expression of memory-associated genes after *AHR* knockout (Fig. 3d). RT-qPCR analysis confirmed that AHR activation by kynurenine in control condition decreased the expression of effector-associated genes such as *TBX21* and *EOMES*, as well as memory-associated genes, including *TCF7* and *SELL*. In clear contrast, and correlating the RNA-sequencing analysis, *AHR* knockout led to an up-regulation of these effector- and memory-associated genes (Fig. 3e). Moreover, flow cytometry analysis of effector cytokine production showed a significant increase in IL-2 producing

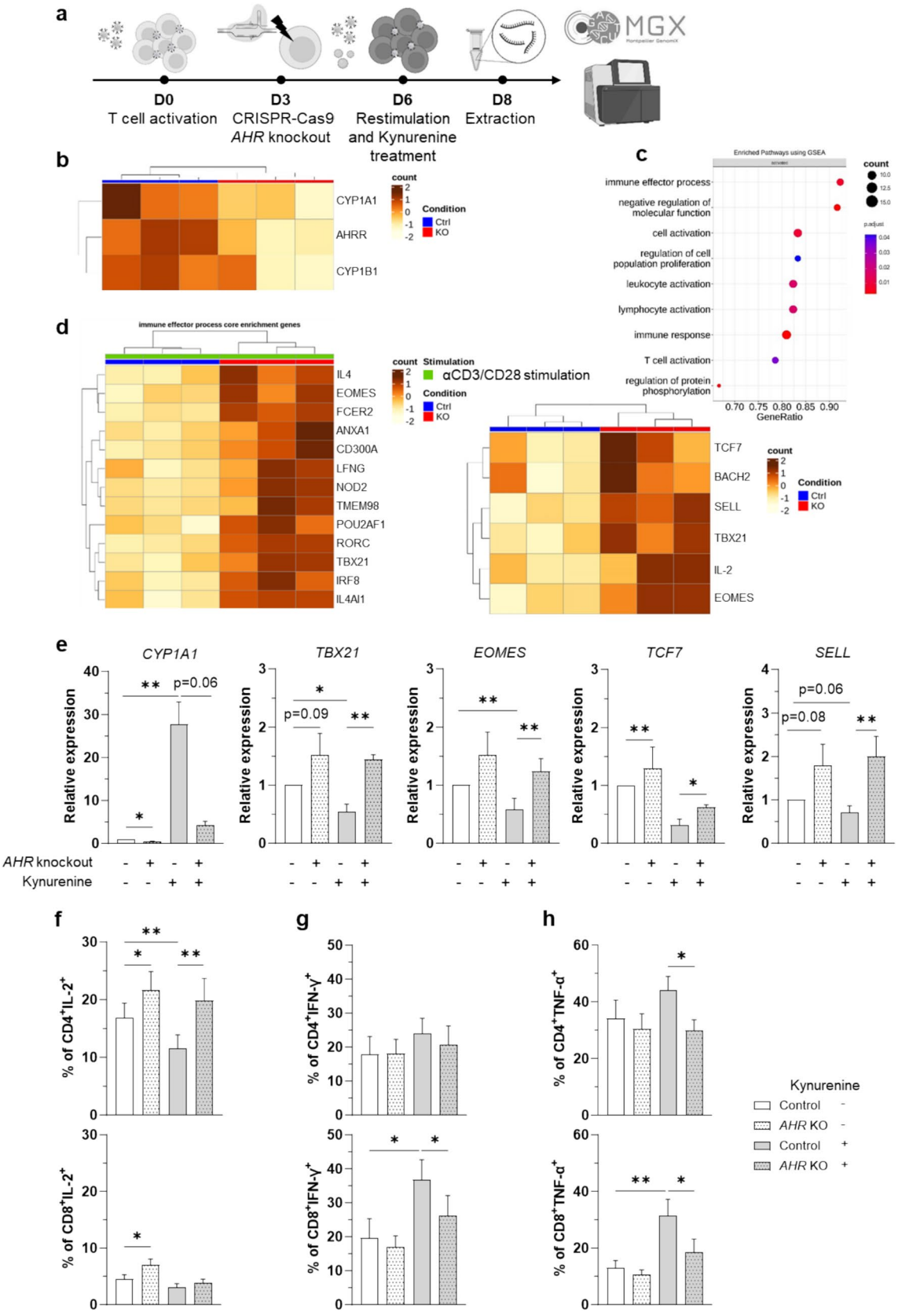
a
D0
T cell activation
D3
CRISPR-Cas9
AHR knockout
D6
Restimulation
and Kynurenine
treatment
D8
Extraction
MGX
b
CYP1A1
AHRR
CYP1B1
count
Condition
Ctrl
KO
c
Enriched Pathways using GSEA
immune effector process
negative regulation of molecular function
cell activation
regulation of cell population proliferation
leukocyte activation
lymphocyte activation
immune response
T cell activation
regulation of protein phosphorylation
GeneRatio
d
immune effector process core enrichment genes
IL4
EOMES
FCER2
ANXA1
CD300A
LFNG
NOD2
TMEM98
POU2AF1
RORC
TBX21
IRF8
IL4AI1
Stimulation
αCD3/CD28 stimulation
TCF7
BACH2
SELL
TBX21
IL-2
EOMES
e
CYP1A1
TBX21
EOMES
TCF7
SELL
Relative expression
p=0.06
p=0.09
p=0.08
AHR knockout
Kynurenine
f
% of CD4+IL-2+
% of CD8+IL-2+
g
% of CD4+IFN-γ+
% of CD8+IFN-γ+
h
% of CD4+TNF-α+
% of CD8+TNF-α+
Kynurenine
Control
AHR KO
Control
AHR KO

◂**Fig. 3** *AHR* knockout promotes effector- and memory-like profiles upon T cell stimulation. **a** Methodology of *AHR* knocked-out T cells' RNA-sequencing. **b** Heatmap showing differential expression of genes regulated by AHR, analyzed using DESeq2. (n = 3) **c** Pathway enrichment analysis using GSEA (Gene Set Enrichment Analysis) based on GO (Gene Ontology) Biological Process. The size of each dot reflects the number of genes contributing to the enrichment of each pathway (count), while the color gradient represents the adjusted *p*-value (*p*.adj), with darker colors indicating higher statistical significance. (n = 3) **d** Heatmap showing differential expression of immune effector and memory genes. (n = 3) **e** RT-qPCR validation of RNA-sequencing data. (n = 5) **f–h** Cytokine analysis of *AHR* knocked-out T cells treated with 50 µM of kynurenine. (n = 11)

cells from 16.8% (S.E.M. ± 2.6) in wild-type T cells to 21.6% (S.E.M. ± 3.6) in *AHR* knocked-out T cells without kynurenine ($p < 0.05$). The same result was observed in presence of kynurenine, with 11.5% (S.E.M. ± 2.4) IL-2 producing wild-type T cells against 19.8% (S.E.M. ± 3.8) for *AHR* knocked-out T cells ($p < 0.01$) (Fig. 3f). Of note, there was a slight decrease in IFN-$\gamma^+$ and TNF-$\alpha^+$ producing T cells (Fig. 3f-h), despite an up-regulation of *TBX21* expression (Fig. 3e).

### *AHR* knockout prevents increased expression of CD39 upon chronic T cell stimulation

The impact of *AHR* knockout on the expression of inhibitory checkpoints genes analyzed by RNA-sequencing showed a down-regulation of *CD101*, *TIGIT* and *ENTPD1* encoding for CD39 (Fig. 4a). An initial focus by flow cytometry on CD39 showed a significant decrease in the percentage of CD39$^+$ T cells going from 51.3% (S.E.M. ± 7.2) to 24.2% (S.E.M. ± 4.2) after *AHR* knockout when treated with kynurenine after chronic stimulation ($p < 0.0001$) (Fig. 4b). The same result was observed for the mean fluorescence of CD39 following *AHR* knockout (Fig. 4c). A downward trend of TIGIT expression and mean of fluorescence was also observed in CD4$^+$ and CD8$^+$ T cells (Fig. 4d,e). Further, immunosuppressive cytokines expression seems to be lower in kynurenine exposed and chronically stimulated T cells (Fig. S1a). Hence, *AHR* knockout seems to limit the impact of chronic stimulation on CD39 expression and to a lesser extent on TIGIT expression. However, no significant differences were observed in the expression of the exhausted markers PD-1 and TIM-3 (Fig. S1b).

### *AHR* knocked-out CAR-T cells are functional

*AHR* knockout was then efficiently applied to a CAR-T model targeting the CD123 antigen (Fig. 5a–c). The knockout did not affect either CAR-T cell cytotoxicity (Fig. 5d) or degranulation capacity (Fig. 5e). As previously observed in T cells, CD39 up-regulation in CD4$^+$ and CD8$^+$ CAR-T cells was prevented by *AHR* knockout (Fig. 5f). Hence, *AHR* knockout is feasible on CAR-T cells without impacting their short-term antitumor capacities.

### *AHR* knocked-out CAR-T cells persist longer than wild type CAR-T cells upon chronic stimulation

A chronic in vitro stimulation assay was then performed on *AHR* knocked-out CAR-T cells to evaluate their long-term antitumoral capacities. CD123$^+$ CAR-T cells were maintained in co-culture with hematologic tumor targets (CAL-1 cell line) in an unfavorable ratio of 1 effector for 15 tumor targets to create a hostile environment through enforced repeated stimulation (Fig. 6a). Every week, remaining CAR-T cells were counted and phenotypically characterized. After 21 days of *AHR* knocked-out CAR-T cells and CAL-1 co-culture, 76.2% (S.E.M. ± 12.2) of remaining cells were *AHR* knocked-out CAR-T cells. In contrast, wild-type CAR-T cells and CAL-1 co-culture led to only 42.6% (S.E.M. ± 14.3) remaining CAR-T cells ($p < 0.05$). Following the fourth round of rechallenge, the beneficial effect of *AHR* knockout on CAR-T cells persistence was still observed, with 57.9% (S.E.M. ± 11.9) of *AHR* knocked-out CAR-T cells persisting compared to 22.9% (S.E.M. ± 9.6) for control CAR-T cells ($p < 0.05$) (Fig. 6b). Hence, *AHR* knocked-out CAR-T cells resisted tumor rechallenge for a longer period of time than wild-type CAR-T cells. Anti-tumor activity of *AHR* knocked-out CAR-T cells has also been assessed with 50 µM kynurenine supplementation and showed that kynurenine supplementation seems to have a negative effect on CD123 CAR-T cells' anti-tumor activity. This effect was not observed when *AHR* is knocked-out (Fig. S2). To characterize the remaining cells, we first evaluated the CD4/CD8 ratio after several rounds of tumor rechallenges. No modification concerning the CD4/CD8 ratio after *AHR* knockout was observed (Fig. 6c). Next, *AHR* knocked-out CAR-T cells were further characterized through the expression of CD39 and TIGIT, previously associated with chronic stimulation (Fig. 1e–g). Weaker frequencies of CD39$^+$ and TIGIT$^+$ of persisting CAR-T cells were observed in the *AHR* knocked-out condition, reinforcing a less dysfunctional state (Fig. 6d, e). These data showed that *AHR* knocked-out CAR-T cells persist longer than CAR-T cells upon chronic stimulation.

## Discussion

Optimizing CAR-T therapy is required to improve its current clinical efficacy and CRISPR-Cas is a suitable tool to identify target involved in T cell dysfunction [3]. Precise gene editing of transcription factors has appeared as a promising approach to target multiple pathways and

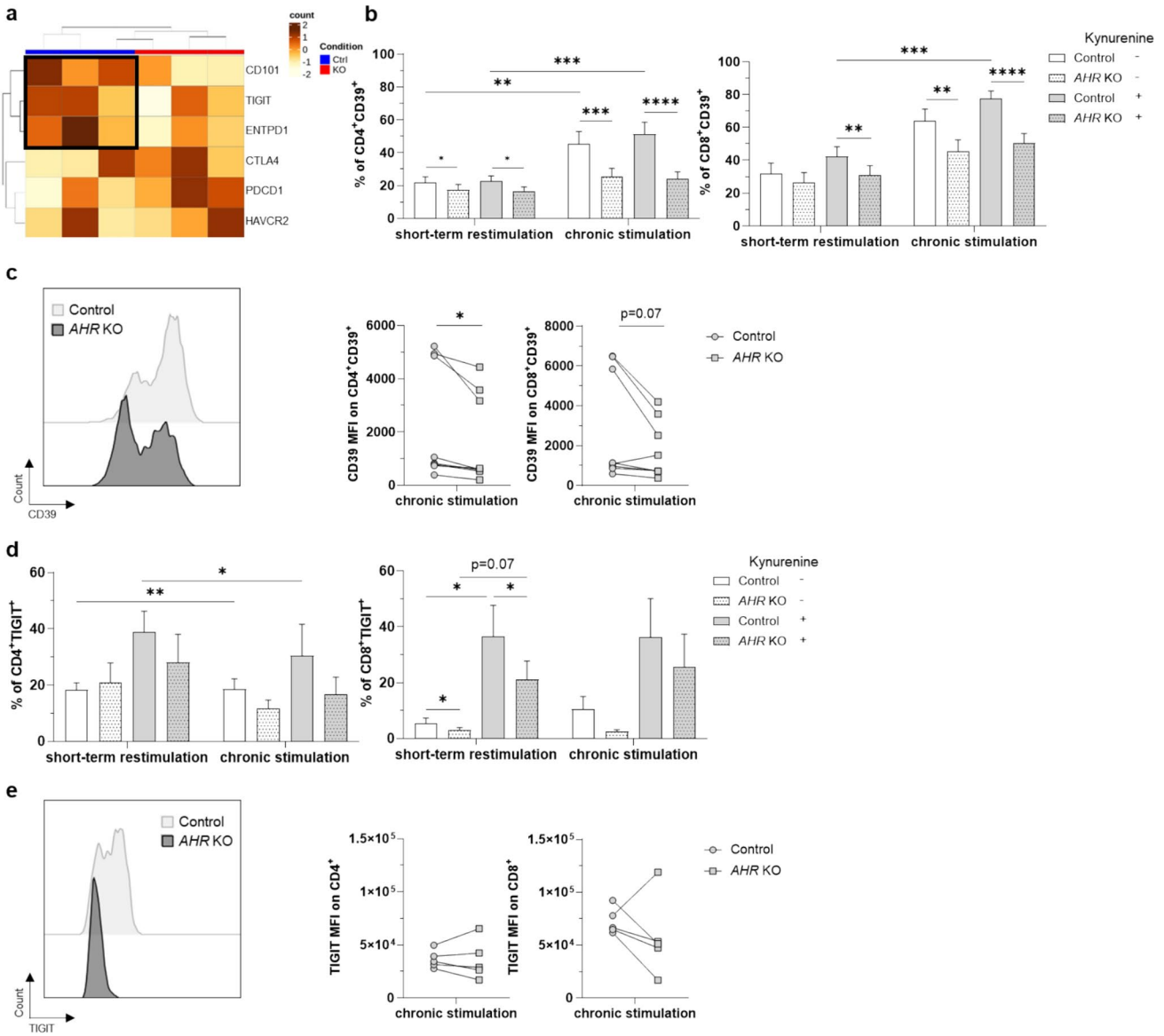


**Fig. 4** *AHR* knockout prevents increased expression of CD39 upon chronic T cell stimulation. **a** Heatmap showing differential expression of inhibitory receptors (n = 3). **b**, **c** CD39 expression (**b**) after short-term restimulation (T cells restimulated once) or chronic stimulation (T cells restimulated four times) in *AHR* knocked-out T cells treated with 50 µM of kynurenine and CD39 mean of fluorescence (**c**) after chronic stimulation (T cells restimulated four times) in CD39.$^{+}$ T cells treated with 50 µM of kynurenine. (n = 13 (**b**), n = 11 (**c**)) **d**, **e** TIGIT expression (**d**) after short-term restimulation or chronic stimulation in *AHR* knocked-out T cells treated with 50 µM of kynurenine and TIGIT mean of fluorescence (**e**) after chronic stimulation (T cells restimulated four times) treated with 50 µM of kynurenine. (n = 10 (**d**), n = 6 (**e**))

factors simultaneously. In this study, we focused on AHR, known for being involved in several biological processes, including immune responses [4]. Being mostly studied in murine model so far, we concentrated our study in human T cells that have yet to be characterized, using the CRISPR-Cas tool.

Many studies were limited by short-term in vitro models, as it does not reflect in vivo conditions. In this study, *AHR* knocked-out T cells were first subjected to an antigen non-specific chronic stimulation based on previous protocols [12, 13]. The aim was to mimic chronic antigen exposure that cells must face in vivo. As expected, chronic stimulation induced a reduction in T cell proliferation capacity and upregulated the expression of several inhibitory receptors, which are hallmarks of dysfunctional T cells. However, it is important to note that inhibitory receptors are expressed not only in exhausted T cells, but also in activated T cells [14]. Hence, heightened inhibitory receptors expression does not

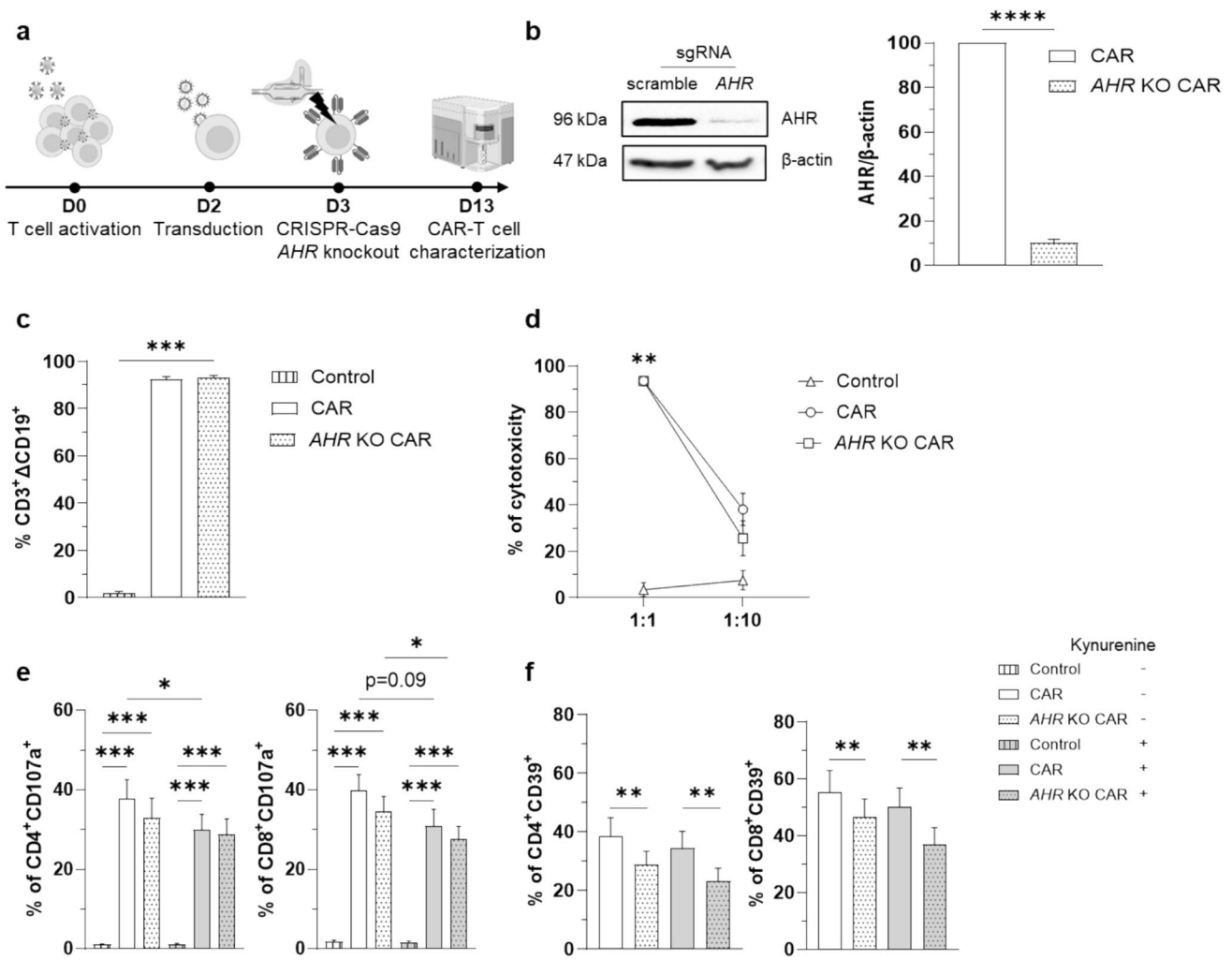


**Fig. 5** *AHR* knocked-out CAR-T cells are functional. **a** Methodology. **b**, **c** Knockout validation (**b**) and transduction efficiency (detected with a percentage of the truncated protein CD19 as a reporter) (**c**) of *AHR* knocked-out CAR-T cells. (n = 14) **d** Cytotoxic assay of *AHR* knocked-out CAR-T cells after co-culture at different effector:target ratios for 24 h. (n = 8 (ratio 1:1), n = 3 (ratio 1:10)) **e** CD107a degranulation assay of *AHR* knocked-out CAR-T cells after co-culture at an effector:target ratio of 1:1 for 5 h treated with 50 µM of kynurenine. (n = 11) **f** CD39 expression in *AHR* knocked-out CAR-T cells after co-culture at an effector:target ratio of 1:1 for 24 h treated with 50 µM of kynurenine. (n = 14)

necessarily mean that T cells are in fact exhausted. Indeed, T cell exhaustion is a complex state that appears after many transcriptomic, epigenetic and metabolic changes caused by many immunosuppressive factors [15]. Hence, this model might not be sufficient to induce permanent dysfunction, since it does not recapitulate all the factors required to induce T cell exhaustion. However, our model can be used as a simple way to study it in vitro. To improve this model, we established a CAR-T chronic stimulation model using tumor cells as targets based on previous protocols [16, 17]. This allowed us to better appreciate *AHR* knockout benefits on CAR-T efficiency.

Engineered T cells were characterized after being treated with the immunosuppressive AHR agonist kynurenine. Surprisingly, kynurenine treatment did not significantly modify wild-type T cell phenotype compared to untreated cells. This might be explained by the plethora of natural ligands that can activate AHR. Indeed, previous studies have shown IL-2 culture conditions induce production of 5-HTP AHR agonist [7]. Moreover, although kynurenine has long been considered a potent agonist of AHR, its structure does not conform to the binding site of the receptor [18]. Another study provided evidence that kynurenine might act as a pro-ligand of AHR, which needs chemical conversions to produce efficient agonists [18, 19]. Kynurenine metabolism has further been involved in ROS production and apoptosis [20, 21] or antioxidant activities [22]. In our in vitro model of stimulated T cells cultured with 50 µM of kynurenine, no significant increase of ROS was observed, in contrast AHR was in fact activated by kynurenine as shown

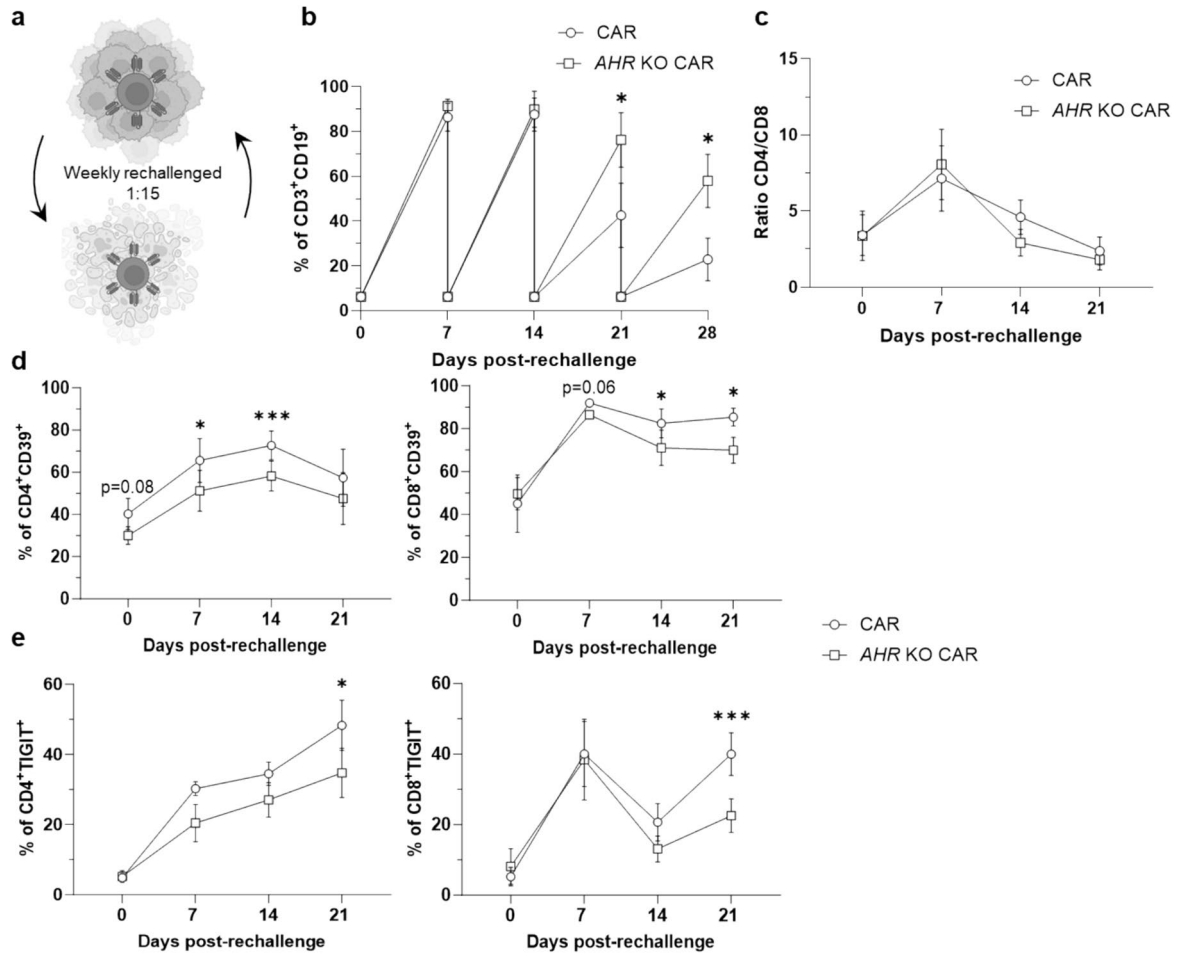


**Fig. 6** *AHR* knockout CAR-T cells persist longer than wild type CAR-T cells upon chronic stimulation. **a** Methodology of in vitro chronic stimulation assay for a hematologic cancer cell line. **b** Follow-up of the percentage of CAR-T remaining after chronic stimulation. (n = 8) **c** CD4 and CD8 ratio upon chronic stimulation. (n = 8) **d**, **e** CD39 and TIGIT expression over time after chronic stimulation in *AHR* knocked-out CAR-T cells. (n = 3)

by AHR nucleus translocation. However, in our model, AHR was in fact activated by kynurenine as shown by AHR nucleus translocation.

In our study, *AHR* knockout enhanced T cell activation capacity and increased the expression of effector- and memory-associated genes as observed with the up-regulation of genes like *TBX21*, *EOMES*, *TCF7* or *BACH2*. These key genes have been described to be involved in potent antitumor responses. Indeed, *TBX21* and *EOMES* genes are characteristics of cytotoxic T cells, while *TCF7* and *BACH2* are characteristics of less differentiated T cells, associated with a better persistence [23–25]. This expression profile might explain the maintained cytotoxicity capacity and the prolonged resistance of *AHR* knocked-out CAR-T cells compared to wild-type CAR-T cells in in vitro chronic stimulation assay.

Phenotypically, engineered T cells exhibited increased IL-2 expression, which is characteristic of a less differentiated profile [26]. This result was expected as AHR was previously described as an inducer of *AIOLOS*, an IL-2 repressor [27]. Moreover, this was also confirmed by another study where *AHR* knockout had been shown to promote a central memory profile rather than resident memory [28]. The latter has been described to play a key role in antitumor immunity with their high cytotoxic capacities [29]. However, in our chronic stimulation model, despite *AHR* knocked-out T cells presenting a less differentiated profile associated with the up-regulation of *TCF7* and *BACH2* in *AHR* knocked-out CAR-T cells exerted potent cytotoxicity.

Moreover, as expected, *AHR* knockout decreased CD39 expression, which has been shown to be associated with an exhausted profile [30]. In addition, transcriptomic analysis also suggested that *AHR* knockout may downregulate other inhibitory receptors such as TIGIT. This is interesting as TIGIT has been identified as highly co-expressed with PD-1 by subsets of $CD8^+$ T cell in cancer patients [31], and its

blocking became a new strategy to optimize T cell antitumor activity by reversing exhaustion [32]. Surprisingly, *AHR* knockout did not decrease PD-1 expression, as previously described [33], but this might be explained by the chronic stimulation leading to an enhanced activation of the cells.

CAR-T chronic stimulation model was also based on previous protocols [16, 17]. Upon chronic stimulation, *AHR* knockout allowed CAR-T cells to persist longer than wild type CAR-T cells, as recently observed with findings on *CD38* targeting [16]. This gene, along with *AHR*, is involved in the immunosuppressive adenosinergic pathway, through CD203a and CD73, and through CD39 and CD73, respectively [34]. In our study, we verified CD39 and CD73 modulation by AHR. However, further investigations are required to precisely define AHR involvement in the adenosine pathway to see if this is the mechanism through which AHR restrains CAR-T cell function.

In summary, this research suggests that AHR would be a valuable target for genetic reprogramming to enhance T cell-based cancer therapies.

**Supplementary Information** The online version contains supplementary material available at https://doi.org/10.1007/s00262-025-04065-5.

**Acknowledgements** MGX acknowledges financial support from France Génomique National infrastructure, funded as part of "Investissement d'Avenir" program managed by Agence Nationale pour la Recherche (contract ANR-10-INBS-09). The figures were created with BioRender.com.

**Author contributions** V.DC. performed the experimental work, analyzed the data and wrote the manuscript. O.Ab., P.M-L. and B.D. assisted in the experimental work. A.D. was involved in the data generation of RNA-sequencing and B.N. performed the analysis. F.GO. provided the CAR construct. Y.G. and R.L. reviewed the manuscript. Y.G. and O.Ad. were involved in the acquisition of funds for the research work. Y.G. supervised the research work.

**Funding** This work was supported by Ligue contre le cancer (no. 2022–0047) and by the BioImp project funded by EU through the European Regional Development Fund of the Region BFC (no. BFC000802).

**Data availability** Data is provided within the manuscript.

## Declarations

**Conflict of interest** The authors declare no competing interests.

**Ethical approval** The studies involving humans were approved by CODECOH (collection agreement number AC-2020-4129). The studies were conducted in accordance with the local legislation and institutional requirements.

**Consent to participate** The participants provided their written informed consent to participate in this study.



## References

1. Tomasik J, Jasiński M, Basak GW (2022) Next generations of CAR-T cells-new therapeutic opportunities in hematology? Front Immunol 13:1034707. https://doi.org/10.3389/fimmu.2022.1034707
2. Good CR et al (2021) An NK-like CAR T cell transition in CAR T cell dysfunction. Cell 184(25):6081–610026. https://doi.org/10.1016/j.cell.2021.11.016
3. De Castro V, Galaine J, Loyon R, Godet Y (2024) Godet et al CRISPR-Cas gene knockouts to optimize engineered T cells for cancer immunotherapy. Cancer Gene Ther. https://doi.org/10.1038/s41417-024-00771-x
4. Gutiérrez-Vázquez C, Quintana FJ (2018) Regulation of the immune response by the aryl hydrocarbon receptor. Immunity 48(1):19–33. https://doi.org/10.1016/j.immuni.2017.12.012
5. Apetoh L et al (2010) The aryl hydrocarbon receptor interacts with c-Maf to promote the differentiation of type 1 regulatory T cells induced by IL-27. Nat Immunol 11(9):854–861. https://doi.org/10.1038/ni.1912
6. Mezrich JD, Fechner JH, Zhang X, Johnson BP, Burlingham WJ, Bradfield CA (2010) An interaction between kynurenine and the aryl hydrocarbon receptor can generate regulatory T cells. J Immunol 185(6):3190–3198. https://doi.org/10.4049/jimmunol.0903670
7. Liu Y et al (2021) IL-2 regulates tumor-reactive CD8+ T cell exhaustion by activating the aryl hydrocarbon receptor. Nat Immunol 22(3):358–369. https://doi.org/10.1038/s41590-020-00850-9
8. Wu D, Wang G, Wen S, Liu X, He Q (2024) ARID5A stabilizes indoleamine 2,3-dioxygenase expression and enhances CAR T cell exhaustion in colorectal cancer. Transl Oncol 42:101900. https://doi.org/10.1016/j.tranon.2024.101900
9. Wang S, Wu J, Shen H, Wang J (2020) The prognostic value of IDO expression in solid tumors: a systematic review and meta-analysis. BMC Cancer 20(1):471. https://doi.org/10.1186/s12885-020-06956-5
10. Liu Y et al (2023) Review immune response of targeting CD39 in cancer. Biomark Res 11(1):63. https://doi.org/10.1186/s40364-023-00500-w
11. Bôle-Richard E et al (2020) CD28/4–1BB CD123 CAR T cells in blastic plasmacytoid dendritic cell neoplasm. Leukemia 34:3228–3241. https://doi.org/10.1038/s41375-020-0777-1
12. Balkhi MY, Wittmann G, Xiong F, Junghans RP (2018) YY1 upregulates checkpoint receptors and downregulates type I cytokines in exhausted, chronically stimulated human T cells. iScience 2:105–122. https://doi.org/10.1016/j.isci.2018.03.009
13. Corselli M, Saksena S, Nakamoto M, Lomas WE, Taylor I, Chattopadhyay PK (2022) Single cell multiomic analysis of T cell exhaustion in vitro. Cytom A 101(1):27–44. https://doi.org/10.1002/cyto.a.24496

14. Fuertes Marraco SA, Neubert NJ, Verdeil G, Speiser DE (2015) Inhibitory receptors beyond T cell exhaustion. Front Immunol 6:310. https://doi.org/10.3389/fimmu.2015.00310
15. Xia A, Zhang Y, Xu J, Yin T, Lu X-J (2019) T cell dysfunction in cancer immunity and immunotherapy. Front Immunol 10:1719. https://doi.org/10.3389/fimmu.2019.01719
16. Veliz K et al (2024) Deletion of CD38 enhances CD19 chimeric antigen receptor T cell function. Mol Ther Oncol 32(2):200819. https://doi.org/10.1016/j.omton.2024.200819
17. Prinzing B et al (2021) Deleting DNMT3A in CAR T cells prevents exhaustion and enhances antitumor activity. Sci Transl Med 13(620):eabh0272. https://doi.org/10.1126/scitranslmed.abh0272
18. Shadboorestan A, Koual M, Dairou J, Coumoul X (2023) The role of the kynurenine/AhR pathway in diseases related to metabolism and cancer. Int J Tryptophan Res 16:11786469231185102. https://doi.org/10.1177/11786469231185102
19. Seok S-H et al (2018) Trace derivatives of kynurenine potently activate the aryl hydrocarbon receptor (AHR). J Biol Chem 293(6):1994–2005. https://doi.org/10.1074/jbc.RA117.000631
20. Song H et al (2011) l-Kynurenine-induced apoptosis in human NK cells is mediated by reactive oxygen species. Int Immunopharmacol 11(8):932–938. https://doi.org/10.1016/j.intimp.2011.02.005
21. Watson MJ, Delgoffe GM (2022) Fighting in a wasteland: deleterious metabolites and antitumor immunity. J Clin Invest. https://doi.org/10.1172/JCI148549
22. González Esquivel D, Ramírez-Ortega D, Pineda B, Castro N, Ríos C, Pérez de la Cruz V (2017) Kynurenine pathway metabolites and enzymes involved in redox reactions. Neuropharmacology 112:331–345. https://doi.org/10.1016/j.neuropharm.2016.03.013
23. Intlekofer AM et al (2005) Effector and memory CD8+ T cell fate coupled by T-bet and eomesodermin. Nat Immunol 6(12):1236–1244. https://doi.org/10.1038/ni1268
24. Yao C et al (2021) BACH2 enforces the transcriptional and epigenetic programs of stem-like CD8+ T cells. Nat Immunol 22(3):370–380. https://doi.org/10.1038/s41590-021-00868-7
25. Zhang J, Lyu T, Cao Y, Feng H (2021) Role of TCF-1 in differentiation, exhaustion, and memory of CD8+ T cells: a review. FASEB J 35(5):e21549. https://doi.org/10.1096/fj.202002566R
26. Zwijnenburg AJ et al (2023) Graded expression of the chemokine receptor CX3CR1 marks differentiation states of human and murine T cells and enables cross-species interpretation. Immunity 56(8):1955-1974.e10. https://doi.org/10.1016/j.immuni.2023.06.025
27. Quintana FJ et al (2012) Aiolos promotes TH17 differentiation by directly silencing Il2 expression. Nat Immunol 13(8):770–777. https://doi.org/10.1038/ni.2363
28. Dean JW, Zhou L (2022) Cell-intrinsic view of the aryl hydrocarbon receptor in tumor immunity. Trends Immunol 43(3):245–258. https://doi.org/10.1016/j.it.2022.01.008
29. Mei X, Li H, Zhou X, Cheng M, Cui K (2022) The emerging role of tissue-resident memory CD8+ T lymphocytes in human digestive tract cancers. Front Oncol 11:819505. https://doi.org/10.3389/fonc.2021.819505
30. Vignali PDA et al (2023) Hypoxia drives CD39-dependent suppressor function in exhausted T cells to limit antitumor immunity. Nat Immunol. https://doi.org/10.1038/s41590-022-01379-9
31. Simon S et al (2020) PD-1 and TIGIT coexpression identifies a circulating CD8 T cell subset predictive of response to anti-PD-1 therapy. J Immunother Cancer 8(2):e001631. https://doi.org/10.1136/jitc-2020-001631
32. Liu L et al (2022) Blocking TIGIT/CD155 signalling reverses CD8+ T cell exhaustion and enhances the antitumor activity in cervical cancer. J Transl Med 20(1):280. https://doi.org/10.1186/s12967-022-03480-x
33. Liu Y et al (2018) Tumor-repopulating cells induce PD-1 expression in CD8+ T cells by transferring kynurenine and AhR activation. Cancer Cell 33(3):480-494.e7. https://doi.org/10.1016/j.ccell.2018.02.005
34. Benton TZ et al (2021) Selective targeting of CD38 hydrolase and cyclase activity as an approach to immunostimulation. RSC Adv 11(53):33260–33270. https://doi.org/10.1039/d1ra06266b